Circle-to-circle constant-thrust orbit raising

Article *in* Journal of the Astronautical Sciences · January 1994

CITATIONS
23

READS
90

2 authors, including:

Salvatore Alfano
Center for Space Standards and Innovation
55 PUBLICATIONS **358** CITATIONS

SEE PROFILE

The Journal of the Astronautical Sciences, Vol. 42, No. 1, January-March 1994, pp. 35–45

Circle-to-Circle Constant-Thrust Orbit Raising

Salvatore Alfano[1] and James D. Thorne[2]

Abstract

This paper provides simple graphical/analytical tools to determine the minimum elapsed time and associated fuel of a constant-thrust vehicle transferring between coplanar circular orbits. The rocket equation models the effects of continuous fuel expenditure while also serving to recast the solution in terms of accumulated velocity change. These orbit-raising solutions are globally mapped with no restrictions on initial thrust magnitude, intermediate eccentricity, or number of revolutions of the central body. Several examples are presented to verify the transfer charts/equations and familiarize the reader with their use. These are useful tools for mission planners and satellite designers to assess preliminary fuel requirements and transfer times for constant-thrust systems. They are also good for performing propulsion trade-off studies for various missions. A straight-edge and scientific calculator are the only tools needed.

Introduction

This paper provides simple graphical/analytical tools for the orbital mission planner to use in designing optimal, coplanar, circle-to-circle, continuous-thrust transfers. Four charts are presented that relate vehicle design parameters to orbit design parameters for orbit raising.

Each transfer is accomplished with constant thrust through the entire flight path with no restriction on its magnitude. The direction of thrust is free to vary within the orbital plane with fuel expenditure modeled by the rocket equation. Although the initial and final orbits are circular, intermediate eccentricity is allowed to grow and shrink for any number of orbit revolutions as optimally determined.

There has been a substantial amount of work done on low-thrust trajectories. Of particular relevance to this paper are the works covering optimal, continuous, low-thrust transfers [1–17]; included in these are numerous papers by Edelbaum [3, 7, 8, 11]. A mission planning tool for optimal, many-revolution, orbit transfer

[1]Chief, Space and Missiles Dynamics Division, Phillips Laboratory, PL/VTA, Kirtland AFB, NM, 87117-6008.

[2]Orbital Dynamics Program Manager, Space and Missiles Dynamics Division, Phillips Laboratory, PL/VTA, Kirtland AFB, NM, 87117-6008.

was presented by Wiesel and Alfano [12] where an analytically derived solution was obtained and presented in graphical form.

The equations of motion used in this optimal control problem are in their complete form for the coplanar circle-to-circle case. The initial acceleration A_i appears in these equations and is allowed to vary from case to case as a parameter. Changing the spacecraft initial acceleration always changes the minimum time to accomplish the orbit raising. To present the solution data in a user-friendly, universal form (Figs. 1–4), the problem is rescaled using the initial orbit radius and gravitational parameter of the central body; in addition, the time-of-flight t_f is replaced by the total accumulated velocity change ν_f. The results of many such optimal cases are presented in graphical form, showing the relationship between spacecraft acceleration, propellant mass fraction, initial-to-final orbit radius ratio, and the minimum accumulated velocity change. The graphs themselves are composed of parametric families of optimal solutions assembled in comprehensive charts for interpolation by the orbital mission planner. Analytical equations are provided when practical.

The charts and equations cover the total range of spacecraft acceleration values. Many users of space assets are interested in minimum-time orbit raising and repositioning, so the high acceleration cases will be of increasing future interest as continuous-thrust propulsion technology improves.

Equations of Motion

The differential equations that define spacecraft motion are derived under the following assumptions: the force of thrust is constant and always in the plane of motion; the vehicle has a fixed propellant mass flow rate; and the vehicle acceleration is due solely to the force of thrust and a spherically symmetric inverse square central gravitational field. The polar equations of motion [18] are

$$\dot{r} = u \tag{1}$$

$$\dot{u} = \frac{v^2}{r} - \frac{\mu}{r^2} + \frac{A_i \sin \phi}{1 + \dot{m}t} \tag{2}$$

$$\dot{v} = -\frac{uv}{r} + \frac{A_i \cos \phi}{1 + \dot{m}t} \tag{3}$$

$$\dot{\theta} = \frac{v}{r} \tag{4}$$

where r is the radial distance of the vehicle from the attracting center, u is the radial velocity component, v is the transverse velocity component, μ is the gravitational constant of the attracting center, A_i is the initial vehicle acceleration, ϕ is the in-plane control angle (measured from the transverse direction to the thrust vector with positive values in the radial direction), and the dot denotes the first derivative with respect to time. The specific propellant mass flow rate $\dot{m}$ is the actual mass flow rate divided by the initial mass; this value is negative when dealing with propellant loss.

Optimal Control Formulation

Given an initial and final radius, the fuel used between circular coplanar orbits must be minimized; this is equivalent to minimizing transfer time because $\dot{m}$

is assumed constant. The control formulation for this problem is taken directly from Bryson and Ho [18] and repeated here for the reader's convenience. The Hamiltonian is written as

$$H = 1 + \lambda_r \dot{r} + \lambda_u \dot{u} + \lambda_v \dot{v} \tag{5}$$

where the polar angle is omitted because the exact initial and final positions are not specified and equations (1–3) do not depend on θ. The behavior of the Lagrange multipliers is given by

$$\dot{\lambda}_r = -\lambda_u\left(-\frac{v^2}{r^2} + \frac{2\mu}{r^3}\right) - \lambda_v\left(\frac{uv}{r^2}\right) \tag{6}$$

$$\dot{\lambda}_u = -\lambda_r + \lambda_v\left(\frac{v}{r}\right) \tag{7}$$

$$\dot{\lambda}_v = -\lambda_u\left(\frac{2v}{r}\right) + \lambda_v\left(\frac{u}{r}\right). \tag{8}$$

The partial of H with respect to the control parameter ϕ must equal zero

$$\frac{\partial H}{\partial \phi} = (\lambda_u \cos\phi - \lambda_v \sin\phi)\frac{A_i}{1 + \dot{m}t} = 0. \tag{9}$$

Knowing the acceleration term cannot be zero, the control law is established as

$$\tan\phi = \frac{-\lambda_u}{-\lambda_v} \tag{10}$$

where $\sin\phi = -\lambda_u/\sqrt{\lambda_v^2 + \lambda_u^2}$ and $\cos\phi = -\lambda_v/\sqrt{\lambda_v^2 + \lambda_u^2}$ [19].

The complete transfer is characterized by the initial choice of Lagrange multipliers. To date, the only closed-form solution that exists is for the many-revolution case where intermediate eccentricity is assumed to be zero and only tangential thrust is considered [3, 12]. Realizing that these multipliers can be scaled without affecting the control law or λ dynamics, λ_r is set to -1 and a numerical search is used to find the remaining two.

Accumulated Velocity Change

Accumulated velocity change v_f is defined here as the total velocity imparted by the force of thrust during the elapsed transfer time t_f,

$$v_f = \int_0^{t_f} \frac{A_i}{1 + \dot{m}t}\, dt. \tag{11}$$

This formulation of the well-known rocket equation serves two purposes: it models the effect of fuel depletion and also defines the relationship between time and thrust-induced velocity change through the equation

$$v_f = \frac{A_i}{\dot{m}} \ln(1 + \dot{m}t_f). \tag{12}$$

Recasting the minimum-time solution in terms of ν_f provides the means for a very compact graphical representation when considering the initial acceleration A_i and the propellant mass fraction,

$$m_p = -\dot{m}t_f \,. \tag{13}$$

Given A_i, m_p, and ν_f the specific mass flow rate and final time are computed as

$$\dot{m} = \frac{A_i}{\nu_f} \ln(1 - m_p) \tag{14}$$

and

$$t_f = -m_p/\dot{m} \,. \tag{15}$$

For the limiting case where $\dot{m}$ and m_p approach zero, the total transfer time from equation (11) is simply

$$t_f = \nu_f/A_i \,. \tag{16}$$

Chart/Equation Generation and Discussion

Proper scaling can eliminate the dependence on a specific central attracting body and allow a global mapping of solutions. The following definitions for distance and time units are based on the initial radial distance r_i and the gravitational parameter of the central body μ:

$$1 \text{ DU}^* = r_i \tag{17}$$

$$1 \text{ TU}^* = \sqrt{r_i^3/\mu} \,. \tag{18}$$

Although these definitions are dependent on the physical parameters of a given transfer, the equations of motion are not. Conveniently, the gravitational parameter is always 1 DU^{*3}/TU^{*2} and the initial values of the (r, u, v) array for any circle-to-circle coplanar transfer are simply (1 DU*, 0 DU*/TU*, 1 DU*/TU*). The final values are (R DU*, 0 DU*/TU*, $\sqrt{1/R}$ DU*/TU*) where R is the ratio of the final radial distance to the initial (r_f/r_i). For this study only orbit raising is considered ($r_f > r_i$).

As previously mentioned, the initial Lagrange multiplier values completely define the transfer. To solve this two-point boundary value problem λ_r is set to -1 and a shooting method [20] is used to find λ_u, λ_v, and t_f. Minimum-time solutions for a variety of orbit ratios and mass fractions are transformed to accumulated velocity change and plotted versus initial acceleration to produce Figs. 1–4. Figure 5 was generated by taking the optimal solutions for Fig. 1 and integrating equation (4) numerically to determine the total polar angle traversed by the vehicle.

The ripples in the curves of Figs. 1–4 reflect a transition region from gravitational force dominance to thrust dominance; they can be used to define the boundaries of low thrust (flat curve), intermediate thrust (rippled curve), and high thrust (constant upward sloping curve). Also, the ripples and subsequent upward slope testify to the additional cost of achieving the final circular condition.

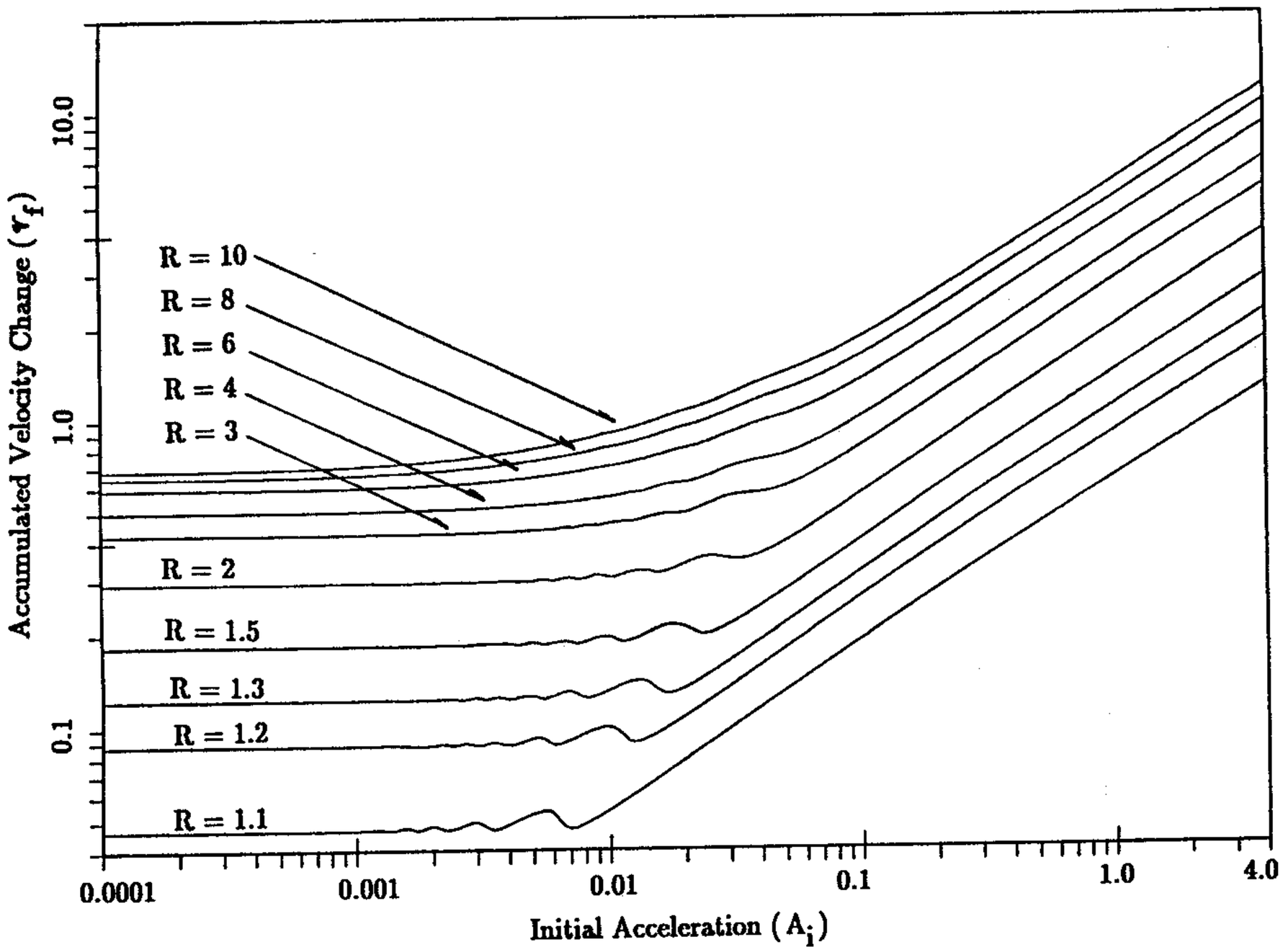

FIG. 1. ν_f Contours for Various Orbit Ratios R $(m_p = 0)$.

As seen in Fig. 5, failure to complete a revolution during transfer increases the associated cost. The optimal steering law causes the eccentricity to increase for the first half of each revolution and then diminish in the latter half: the greater the thrust, the greater the eccentricity increase. If the total polar angle is not a multiple of 2π, the eccentricity must be zeroed out to meet the final condition of a circular orbit; the additional cost of this process is reflected by the peaks in the curves. When making more than five revolutions of the central body this effect is negligible because the induced eccentricity is very small and correctable with little additional maneuvering. If the final state is reached in less than one revolution, the intermediate eccentricity and associated cost grow with the shortness of the transfer arc. This is reflected in the positive slope of the curves. The cost of re-circularization diminishes as the ratio R increases because the gravitational force is less, making vehicle acceleration more effective. Also, when compared to Fig. 1, the smaller ripples of Figs. 2–4 reflect the increased thrust effectiveness due to mass loss.

Wiesel and Alfano [12] characterized all continuous-thrust circle-to-circle transfers where $A_i < 10^{-4}$ DU*/TU*^{2} due to the constancy of accumulated velocity change for a given orbit ratio. The equation relating orbit radius r to velocity change ν for coplanar transfers [12] reduces to

$$\frac{dr}{d\nu} = 2\sqrt{\frac{r^3}{\mu}}. \tag{19}$$

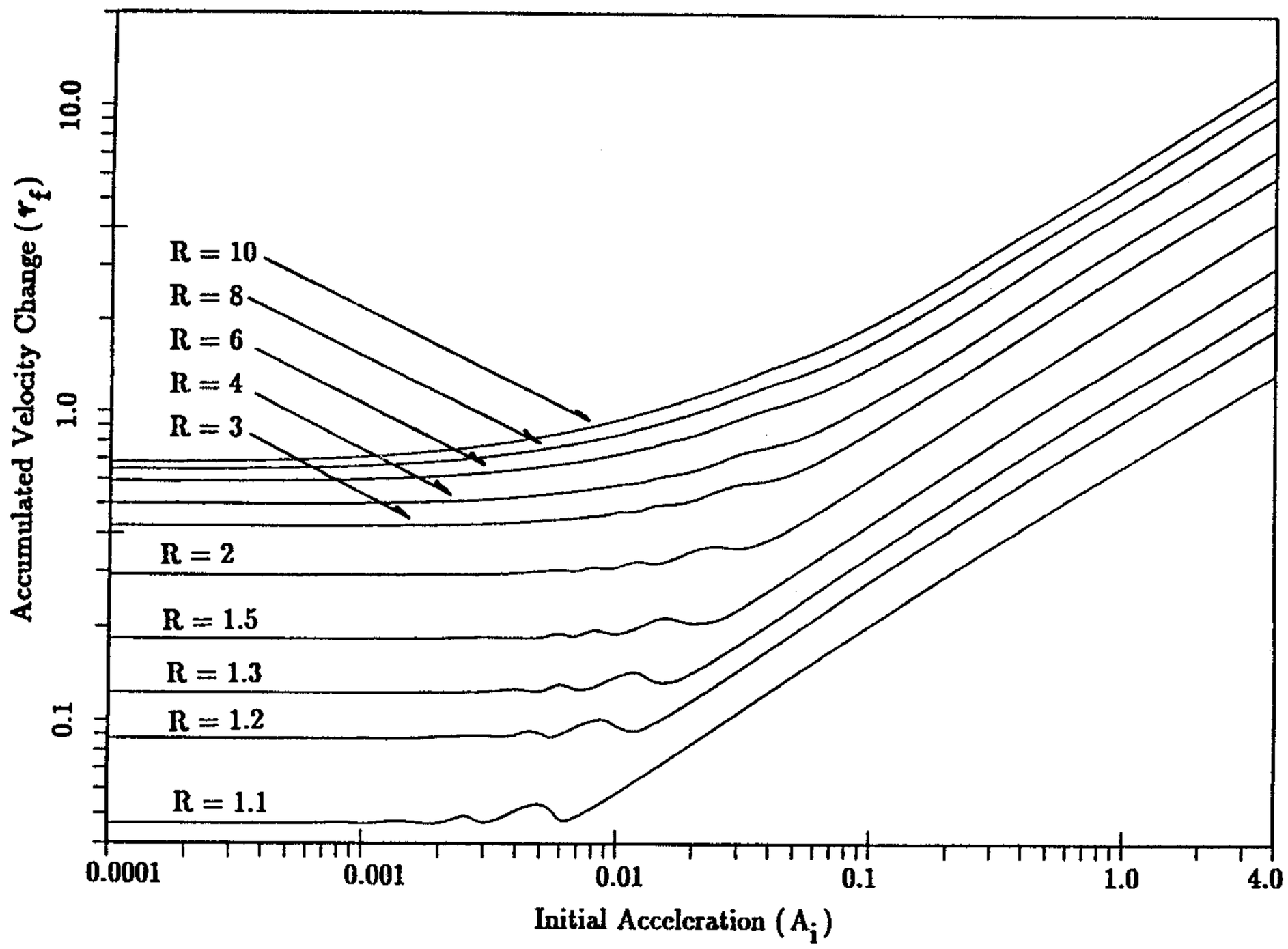

FIG. 2. ν_f Contours for Various Orbit Ratios R $(m_p = 0.25)$.

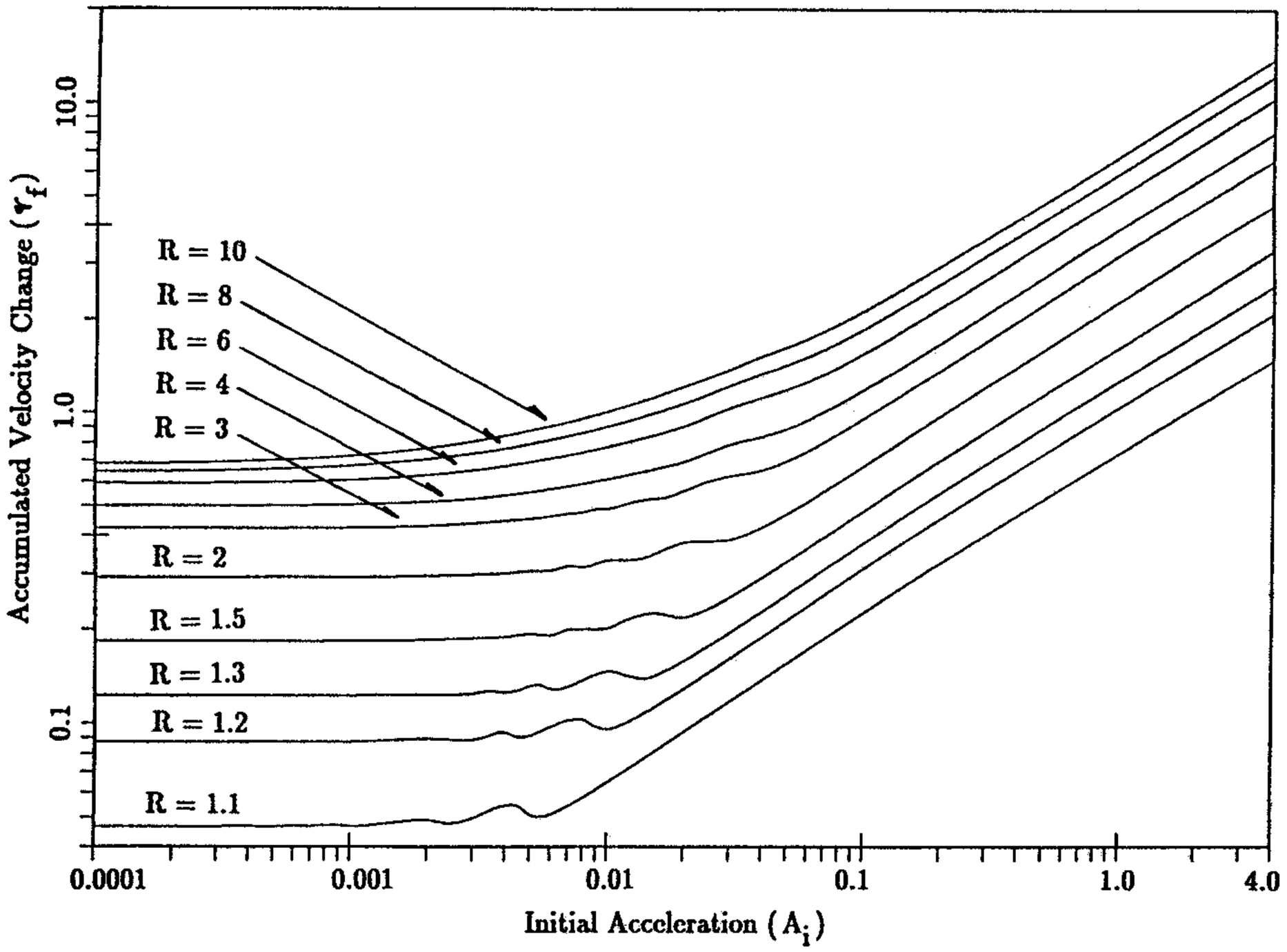

FIG. 3. ν_f Contours for Various Orbit Ratios R $(m_p = 0.5)$.

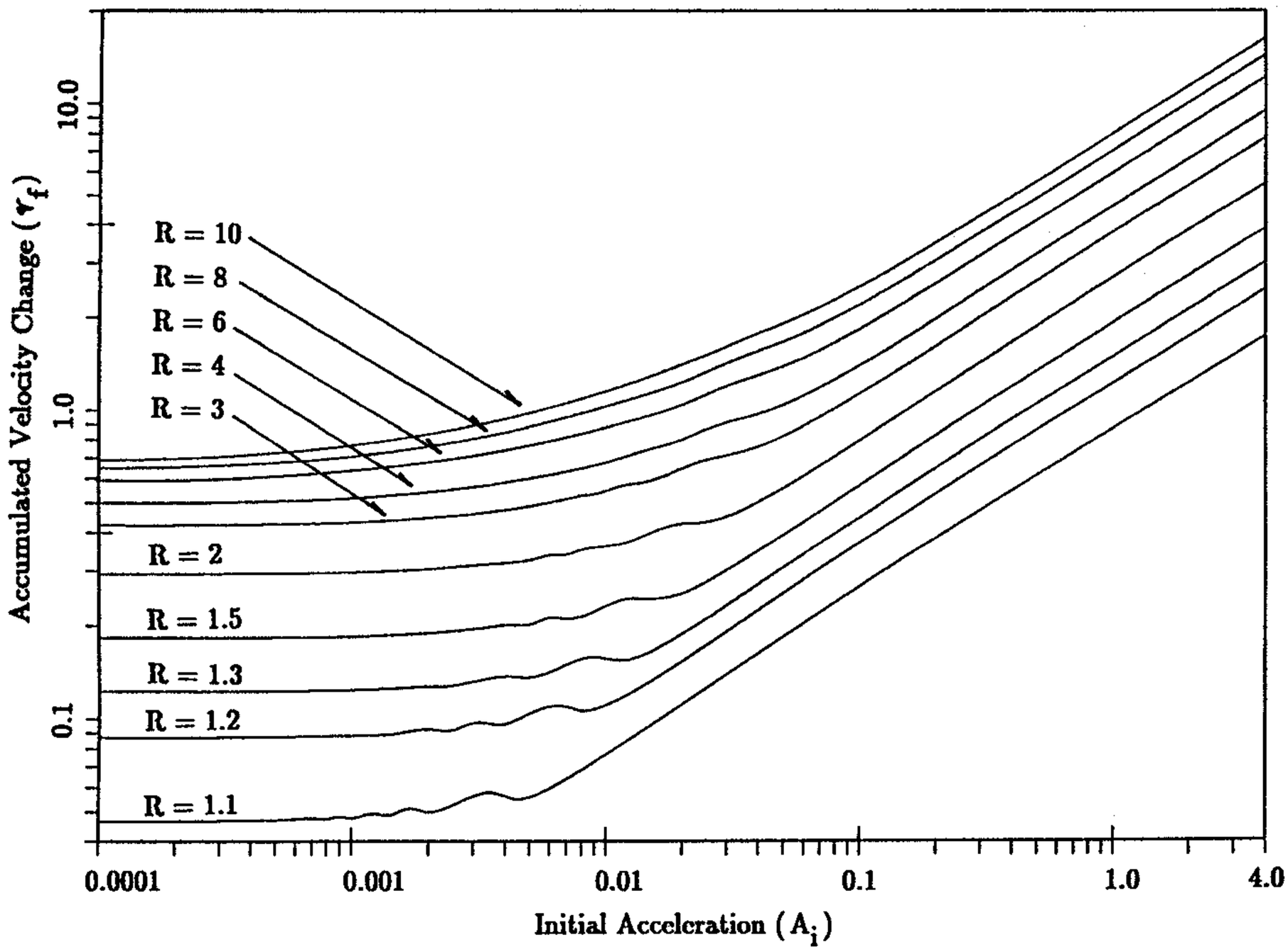

FIG. 4. ν_f Contours for Various Orbit Ratios R $(m_p = 0.75)$.

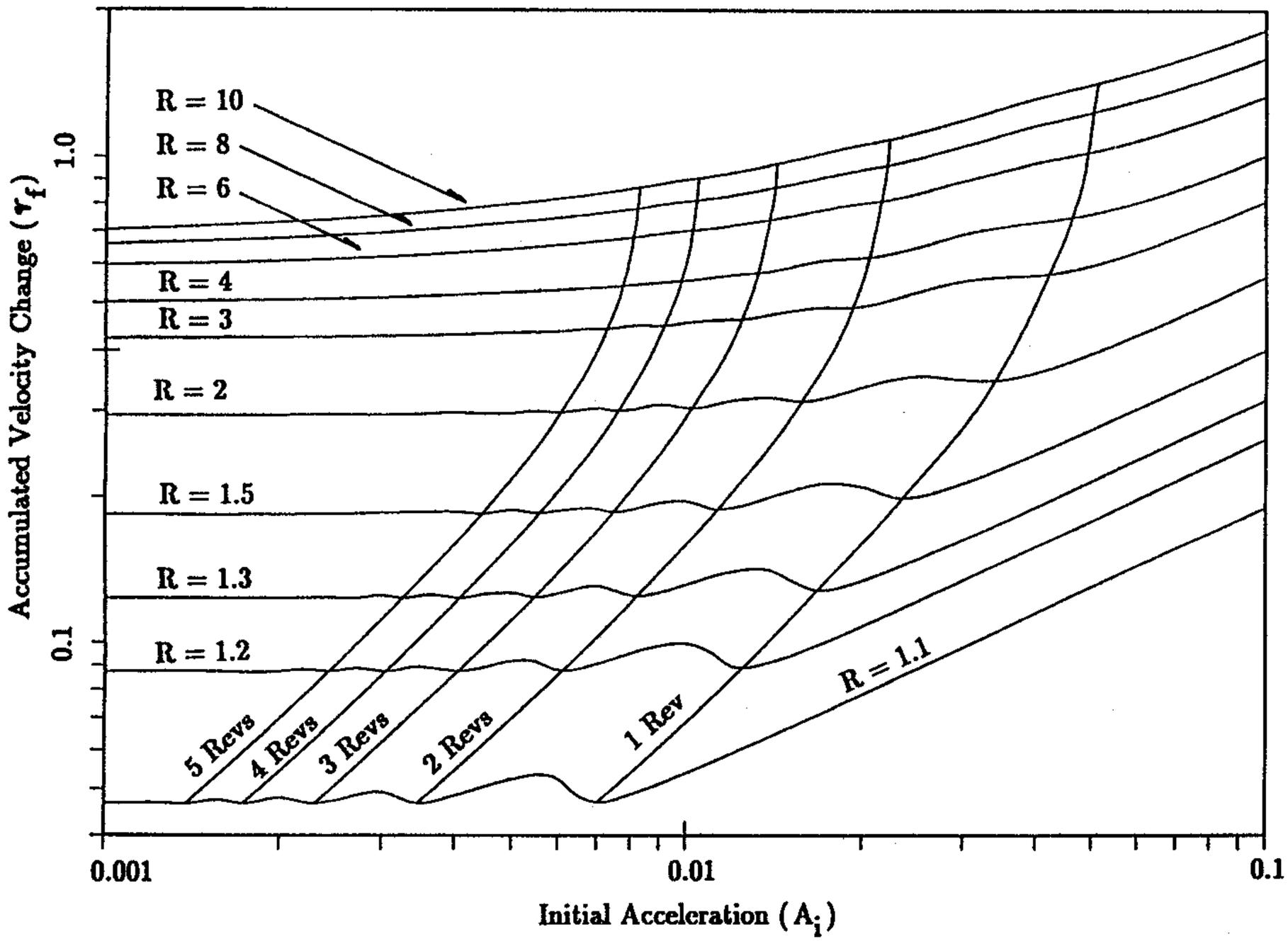

FIG. 5. ν_f Contours with Superimposed Revolution Lines $(m_p = 0)$.

Using the previously defined units and boundary conditions, the accumulated velocity change for orbit-raising is simply

$$v_f = 1 - \sqrt{\mu/R}\,. \tag{20}$$

The constant upward sloping lines in Figs. 1–4 are analytically determined by examining the limiting high-thrust case; the gravitational force is dwarfed by the thrust and assumed negligible. This results in a straight-line radial trajectory where acceleration is directly away from the central body until the switching time t_s, then it is reversed to complete the transfer. All transfers where $A_i > 4$ can be approximated by the equation

$$v_f = 2\sqrt{(R-1)A_i}, \quad (m_p = 0) \tag{21a}$$

or

$$v_f = -\ln(1-m_p)\sqrt{\frac{(R-1)A_i}{2-m_p-2\sqrt{1-m_p}}}, \quad (m_p > 0)\,. \tag{21b}$$

The final time is found from equation (15) or (16) and the switching time is

$$t_s = 0.5\,t_f, \quad (m_p = 0) \tag{22a}$$

or

$$t_s = \left(\frac{1-\sqrt{1-m_p}}{m_p}\right)t_f, \quad (m_p > 0)\,. \tag{22b}$$

Chart/Equation Verification and Use

As a matter of convention, the input parameters will always be given as the array $(r_i, r_f, \mu, A_i, m_p)$. It is assumed the reader can determine total accumulated velocity to two significant figures from the transfer charts; six significant figures will be carried in all computations to reduce round-off error. Physical constants can be found in Seidelmann [21]. The data will be presented in the following form:

a) Unscaled Input Array
b) Scaled Input Array (equations (17) and (18))
c) Accumulated velocity change from appropriate chart or equation
d) Mass flow rate (equation (14), if needed)
e) Minimum time-of-flight (equation (15) or (16)).

Test Case 1

The first test case is an Earth-Mars transfer where both planetary orbits are assumed to be circular and coplanar. The spacecraft starts in a heliocentric orbit free of Earth's gravitational field and finishes free of Mars' field; Earth escape and Mars capture are not considered. An Earth-Mars transfer solution can be found in Bryson and Ho [18], but a mass flow rate of -12.9 lb/day is given for a 10^4 lb vehicle instead of the propellant mass fraction required here; interpolation will be needed to find a solution. The specific mass flow rate is -1.29×10^{-3}/day or -1.49306×10^{-7}/s; as a starting point m_p is set at 0.25.

a) (1.49598×10^{11} m, 2.27939×10^{11} m, $1.32712\times$ m^3/s^2, 8.33173×10^{-4} m/s^2, 0.25)

b) (1.0 DU*, 1.52368 DU*, 1.0 DU^{*3}/TU^{*2}, 0.1405 DU^*/TU^{*2}, 0.25)
c) $v_f = 0.54$ DU*/TU* (from Fig. 2)
d) $\dot{m} = -0.0748506/TU^* = -1.49026 \times 10^{-8}/s$
e) $t_f = 3.33999$ TU* $= 1.67756 \times 10^7$ s

This final time solution is adequate because $\dot{m}$ from equation (14) is within two significant figures of the original. For illustration purposes, m_p will be increased to 0.5 and interpolation will be used to refine the results and better determine the transfer time.

a) (1.49598×10^{11} m, 2.27939×10^{11} m, 1.32712×10^{20} m^3/s^2, 8.33173×10^{-4} m/s^2, 0.5)
b) (1.0 DU*, 1.52368 DU*, 1.0 DU^{*3}/TU^{*2}, 0.1405 DU^*/TU^{*2}, 0.5)
c) $v_f = 0.59$ DU*/TU* (from Fig. 3)
d) $\dot{m} = -0.165063/TU^* = -3.28637 \times 10^{-8}/s$
e) $t_f = 3.02915$ TU* $= 1.52144 \times 10^7$ s.

Linear interpolation of $\dot{m}$ produces a final time of 3.33951 TU*, 1.67729×10^7 s, or 194.131 days. This is within two significant figures of the Bryson and Ho solution of 193 days [18] and the exact numerical solution of 192.748 days.

Test Case 2

This case involves a LEO-GEO coplanar transfer from a circular parking orbit of 1.05 $DU_\oplus$ to a final circular orbit of 6.61 $DU_\oplus$. The initial vehicle acceleration is 4.0×10^{-6} m/s^2 with a propellant mass fraction of 0.25.

a) (1.05 $DU_\oplus$, 6.61 $DU_\oplus$, 1.0 $DU_\oplus^3/TU_\oplus^2$, 4.0×10^{-6} m/s^2, 0.25)
b) (1.0 DU*, 6.29524 DU*, 1.0 DU^{*3}/TU^{*2}, 4.50079×10^{-7} DU^*/TU^{*2}, 0.25)
c) $v_f = 0.60144$ DU*/TU* (from equation (20))
d) $\dot{m} = -2.15282 \times 10^{-7}/TU^* = -2.48 \times 10^{-10}/s$
e) $t_f = 1.16126 \times 10^6$ TU* $= 1.00806 \times 10^9$ s.

This case involves low thrust (flat curve for Figs. 1–4, v_f constant for a given orbit ratio R regardless of m_p or A_i) and agrees with the numerical solution.

Test Case 3

This is a high-thrust LEO-GEO transfer similar to case 2 with the acceleration increased by a factor of 10^8 and a propellant mass fraction of 0.75.

a) (1.05 $DU_\oplus$, 6.61$DU_\oplus$, 1.0 $^3_\oplus/TU_\oplus^2$, 4.0×10^2 m/s^2, 0.75)
b) (1.0 DU*, 6.29524 DU*, 1.0 DU^{*3}/TU^{*2}, 45.0079 DU^*/TU^{*2}, 0.75)
c) $v_f = 42.80285$ DU*/TU* (from equation (21b))
d) $\dot{m} = -1.45771/TU^* = -1.67925 \times 10^{-3}/s$
e) $t_f = 0.514505$ TU* $= 446.628$ s.

The exact numerical solution is 445.582 s.

Closing Remarks

This paper provides simple graphical/analytical tools to determine the minimum elapsed time and associated fuel of a constant-thrust vehicle for circle-to-circle coplanar transfers. Accumulated velocity change replaces the time-of-flight while also accounting for propellant mass loss. The solutions are globally mapped with no restrictions on initial thrust magnitude, intermediate eccentricity, or number of revolutions of the central body. Several examples are presented that verify the

transfer charts/equations and show their ease of use. These are useful tools for mission planners and satellite builders to assess preliminary fuel/time requirements or to compare different propulsion technologies. No computer is needed for analysis, only a straight-edge and a scientific calculator.

Figures 1–4 were designed for preliminary fuel/time assessment and do not portray the associated control history of the thrust angle ϕ. The numerical solutions are very sensitive to small changes of the initial Lagrange multipliers; charts of multipliers could not be read with sufficient accuracy, so none were included in this paper. Also, because this paper deals with preliminary design, charts of initial thrust angles were not included. A method to determine the thrust vectoring strategy analytically or semi-analytically will be the subject of a future paper.

A Hohmann-like transfer will always be more fuel efficient than a continuous-thrust transfer; this could be accomplished by a series of near-impulsive thrusting segments at a predetermined periapsis followed by a similar sequence at the corresponding apoapsis. Two advantages of continuous thrusting are shorter transfer times and reduced on-off cycling of the propulsion system. The charts and equations given here are well suited for such trade-off studies.

References

[1] LEVIN, E. "Low-Thrust Transfer Between Circular Orbits," Paper No. 59-AV-2, ASME Aviation Conference, Los Angeles, California, March 1959.

[2] FAULDERS, C. R. "Optimum Thrust Programming of Electrically Powered Rocket Vehicles in a Gravitational Field," *ARS Journal,* Vol. 30, No. 10, October 1960, pp. 954–960.

[3] EDELBAUM, T. N. "Propulsion Requirements for Controllable Satellites," *ARS Journal,* Vol. 31, August 1961, pp. 1079–1089.

[4] MELBOURNE, W. G. "Three-Dimensional Optimum Thrust Trajectories for Power Limited Propulsion Systems," *ARS Journal,* Vol. 31, No. 12, December 1961, pp. 1723–1728.

[5] LINDORFER, W., and MOYER, H. G. "Application of a Low Thrust Trajectory Optimization Scheme to Planar Earth-Mars Transfer," *ARS Journal,* Vol. 32, No. 2, February 1962, pp. 260–262.

[6] FAULDERS, C. R. "Optimum Thrust Programming of Electrically Powered Rocket Vehicles for Each Escape," *AIAA Journal,* Vol. 1, No. 1, January 1963, pp. 233–234.

[7] EDELBAUM, T. N. "Optimum Low-Thrust Rendezvous and Station Keeping," *AIAA Journal,* Vol. 2, No. 7, July 1964, pp. 1196–1201.

[8] EDELBAUM, T. N. "Optimum Power-Limited Orbit Transfer in Strong Gravity Fields," *AIAA Journal,* Vol. 3, No. 5, May 1965, pp. 921–925.

[9] SHI, Y. Y., and ECKSTEIN, M. C. "Ascent or Descent from Satellite Orbit by Low Thrust," *AIAA Journal,* Vol. 4, December 1966, pp. 2203–2209.

[10] ECKSTEIN, M. C., and SHI, Y. Y. "Low Thrust Elliptical Spiral Trajectories of a Satellite with Variable Mass," *AIAA Journal,* Vol. 5, August 1967, pp. 1491–1494.

[11] EDELBAUM, T. N., SACKETT, L. L., and MALCHOW, H. L. "Optimal Low Thrust Geocentric Transfer," Paper No. 73-1074, AIAA 10th Electric Propulsion Conference, Lake Tahoe, Nevada, October-November 1973.

[12] WIESEL, W. E., and ALFANO, S. "Optimal Many-Revolution Orbit Transfer," *Journal of Guidance,* Vol. 8, No. 1, January-February 1985, pp. 155–157.

[13] KECHICHIAN, J. A. "Low Thrust Eccentricity Constrained Orbit Raising," Paper No. 91-156, AAS/AIAA Spaceflight Mechanics Meeting, Houston, Texas, February 1991.

[14] BROUCKE, R. A. "Low-Thrust Trajectory Optimization in an Inverse Square Force Field," Paper No. 91-159, AAS/AIAA Spaceflight Mechanics Meeting, Houston, Texas, February 1991.

[15] BAUER, T. A. "Near-Optimum Low-Thrust Transfer in Semi-Major Axis and Eccentricity," Paper No. 92–134, AAS/AIAA Spaceflight Mechanics Meeting, Colorado Springs, Colorado, February 1992.

[16] BURTON, R. L., and WASSGREN, C. "Time-Critical Low-Thrust Orbit Transfer Optimization," *Journal of Spacecraft and Rockets,* Vol. 29, No. 2, March-April 1992, pp. 286–288.
[17] PRUSSING, J. E. "Equation for Optimal Power-Limited Spacecraft Trajectories," Paper No. 93-147, AAS/AIAA Spaceflight Mechanics Meeting, Pasadena, California, February 1993.
[18] BRYSON, A. E., and HO, Y. *Applied Optimal Control,* Hemisphere Publishing Corporation, Washington, D.C., 1975, pp. 42–89.
[19] WOOD, L. J. "Comment on 'Application of the Conjugate Gradient Method to a Problem on Minimum Time Orbit Transfer'," *IEEE Transactions on Aerospace and Electronic Systems,* Vol. AES-13, No. 4, July 1977, pp. 388–390.
[20] PRESS, W. H., TEUKOLSKY, S. A., VETTERLING, W. T., and FLANNERY, B. P. *Numerical Recipes in Fortran,* Cambridge University Press, Cambridge, 1992, pp. 749–751.
[21] SEIDELMANN, P. K. (editor) *Explanatory Supplement to the Astronomical Almanac,* University Science Books, California, 1992, pp. 696, 704.